Progress in Polymer Science 103 (2020) 101222

Contents lists available at ScienceDirect

Progress in Polymer Science

journal homepage: www.elsevier.com/locate/ppolysci

Polymer design to promote low work function surfaces in organic electronics

Yao Wu [b], Yao Liu [a,*], Todd Emrick [b,**], Thomas P. Russell [a,b,*]

[a] Beijing Advanced Innovation Center for Soft Matter, Science and Engineering, State Key Laboratory of Chemical Resource Engineering, Beijing University of Chemical Technology, Beijing, 100029, China
[b] Polymer Science and Engineering Department, University of Massachusetts Amherst, 120 Governors Drive, Amherst, MA, 01003, USA

ARTICLE INFO

Article history:
Available online 15 February 2020

Keywords:
Interface engineering
Polymer interlayers
Organic photovoltaics
Organic light-emitting diodes
Organic field-effect transistors

ABSTRACT

Organic electronics (OEs) are advantageous for their mechanical flexibility, light weight, and easy solution processability over large areas, all ideal characteristics for next generation portable, cost-effective flexible electronics. The interlayer materials present between the organic active layer and electrodes are critical elements for promoting efficient device operation. Recently, solution-processable polymers have been investigated extensively as efficient electrode interlayer materials for applications in OE devices. We begin this article by describing energy level alignment mechanisms associated with contact of the polymer interlayer and metal electrode. We then overview the latest progress where polymer interlayer materials are used in efficient OE device fabrication. We discuss critical properties of these polymer interlayers, including (1) polymer interactions with the metal surface; (2) the effect of energy levels and electronic structures of these polymers on interfacial modification; and (3) the effect of charge transport and conductivity of the polymer interlayer on device operation. Our motivation is to describe our current understanding, recent progress, and outstanding issues of polymer interlayers in OEs, and propose future potential directions and opportunities.

Published by Elsevier B.V.

Abbreviations: Au, Gold; BHJ, Bulk Heterojunction; CPE, Conjugated Polymer Electrolytes; CPZ, Conjugated Polymer Zwitterion; D-A, Donor-Acceptor; DPP, Diketopyrrolopyrrole; *Eg*, Energy Gap; ESR, Electron Spin Resonance; *FF*, Fill Factor; HOMO, Highest Occupied Molecular Orbital; ICT, Integer Charge Transfer; *i*In, *iso*-indigo; ITO, Indium Tin Oxide; J_{SC}, Short Circuit Current Density; LUMO, Lowest Unoccupied Molecular Orbital; MEH-PPV, Poly[2-methoxy-5-(2-ethylhexyloxy)-1,4-phenylenevinylene]; N2200, Poly[[N,N′-bis(2-octyldodecyl)-naphthalene-1,4,5,8-bis(dicarboximide)-2,6-diyl]-alt-5,5-(2,2′-bithiophene)]; NDI, Naphthalene Diimide; NEXAFS, Near-Edge X-Ray Absorption Fine Structure; OE, Organic Electronic; OFET, organic field-effect transistors; OLED, Organic Light-Emitting Diode; OPV, Organic Photovoltaic; P3TMAHT, Poly[3-(6-trimethylammoniumhexyl) thiophene]; PBDTT-TT, Poly([2,6′-4,8-di(5-ethylhexylthienyl)benzo[1,2-b;3,3-b]dithiophene][3-fluoro-2[(2-ethylhexyl)carbonyl]thieno[3,4-b]thiophenediyl]); $PC_{71}BM$, [6,6]-phenyl-C_{71}-butyric acid methyl ester; PCDTBT, Poly[N-9″-heptadecanyl-2,7-carbazole-alt-5,5-(4′,7′-di-2-thienyl-2′,1′,3′-benzothiadiazole)]; PCE, Power Conversion Efficiency; PDI, Perylene Diimide; PDPPNBr, Poly-2,5-bis(2-octyldodecyl)-3,6-bis(thiophen-2-yl)-pyrrolo[3,4-c]pyrrole-1,4-dione-alt-2,5-bis[6-(*N,N*,N-trimethylammonium)hexyl]-3,6-bis(thiophen-2-yl)-pyrrolo[3,4-c]pyrrole-1,4-dione; PEDOT: PSS, Poly(3,4-ethylenedioxythiophene): poly(styrenesulfonic acid); PEI, Polyethylenimine; PEIE, Poly(ethylenimine ethoxylated); PEO, Polyethylene oxide; PF2/6-*b*-P3TMAHT, Poly(9,9-bis(2-ethylhexyl)-fluorene]-b-poly[3-(6-trimethylammonium-hexyl)thiophene]; PF-EP, Poly(9, 9-bis (60-diethoxylphosphorylhexyl) fluorene; PFN, Poly[(9,9-bis(3′-(*N,N*-dimethylamino)propyl)-2,7-fluorene)-alt-2,7-(9,9–dioctylfluorene)]; PFN-OH, Poly[9,9-bis(6′-(diethanolamino)hexyl)-fluorene]; PFN-OX, Poly[9,9-bis(6′-(*N,N*-diethylamino)propyl)-fluorene-alt-9,9-bis-(3-ethyl(oxetane-3-ethyloxy)-hexyl)-fluorene]; PN4N, Amino-Functionalized Polymer Dopant; PNDIT-F3N, Poly[(9,9-bis(3′-(*N,N*-dimethylamino)propyl)-2,7-fluorene)-alt-5,5′-bis(2,2′-thiophene)-2,6-naphthalene1,4,5,8-tetracaboxylic-*N,N*′-di(2-ethylhexyl)imide]; PNDIT-F3N-Br, Poly[(9,9-bis(3 ′-((*N,N*-dimethyl)-Nethylammonium)propyl)-2,7-fluorene)-alt-5,5′-bis(2,2′-thiophene)-2,6-naphthalene-1,4,5,8-tetracaboxylic-*N,N*′-di(2-ethylhexyl)imide]-dibromide; SB, Sulfobetaine; SCLC, Space Charge Limited Current; UPS, Ultraviolet Photoelectron Spectroscopy; V_{bi}, Built-In Electric Field; V_{OC}, Open Circuit Voltage; VR-SFG, Vibrational Resonant Sum Frequency Generation; WPF-6-oxy-F, Poly[(9,9-bis((60-(*N,N*,N-trimethylammonium)hexyl)-2,7-fluorene)-alt-(9,9-bis(2-(2-(2-methoxyethoxy)ethoxy)ethyl)-9-fluorene)) dibromide; Φ_e, Electron Injection Barrier; μ_e, Electron Mobility.

* Corresponding authors at: Beijing Advanced Innovation Center for Soft Matter, Science and Engineering, State Key Laboratory of Chemical Resource Engineering, Beijing University of Chemical Technology, Beijing, 100029, China.
** Corresponding author at: Polymer Science and Engineering Department, University of Massachusetts Amherst, 120 Governors Drive, Amherst, MA, 01003, USA.
E-mail addresses: liuyao@mail.buct.edu.cn (Y. Liu), tsemrick@mail.pse.umass.edu (T. Emrick), russell@mail.pse.umass.edu (T.P. Russell).

https://doi.org/10.1016/j.progpolymsci.2020.101222
0079-6700/Published by Elsevier B.V.

Contents

1. Introduction

State-of-the-art organic electronic and optoelectronic devices, e.g. OFETs, OLEDs, and OPVs, are complex multilayered structures [1–6]. Synthetic tailoring of the chemical structure of organic semiconductors in device active layers offers a distinct advantage in the rational development of materials for organic electronics (OEs) and efficient device performance [7–10]. Supported by decades of fundamental research, organic semiconductors with remarkable properties have been developed. For examples, ambipolar charge carrier mobilities in excess of 10 $cm^2/V{\cdot}s$ and large on/off ratios, have been reported for OFETs [11–13]. High power efficiencies were demonstrated for white and monochromatic OLEDs [14–16]. Moreover, the PCEs of single-junction OPVs and in tandem device architectures now exceed 16 % [17] and 17 % [18], respectively. Although such advances bring the concepts of organic optoelectronic devices closer to commercial viability, the unique competitive advantage of organic materials is found in the potential cost-effectiveness of solution-based processing of high-throughput, large-area devices. Emerging application areas will exploit the light weight, mechanical flexibility, and semi-transparency of OE devices [19].

The interlayer materials that are placed between the organic active layer and charge-collecting electrodes are critical elements in the operation of OE and optoelectronic devices [20,21]. Interlayers reduce the Schottky barrier height, improving charge injection in OFETs and OLEDs [22,23]. In OPVs, the interlayers increase the V_{bi} in the device active layer, ensuring efficient extraction of photo-generated charge carriers [24]. Inorganic interlayers that require vacuum deposition or high-temperature annealing as device fabrication steps limit scalability and compatibility with high-throughput, energy-efficient, large-area solvent-processing, especially on polymeric substrates which have desirable flexible properties [25,26]. Hence, replacing transition metal oxides (ZnO, TiO_2, and MoO_3), metal salts (LiF) and low-work-function metals (Ca, Ba, and Al) to realize "all-organic" device architectures is highly desirable [27]. As such, interface engineering, i.e. the development of interlayer materials and their integration into devices, is now recognized as a critically important research area for realizing OEs as a practical technology [28,29].

Solution-processed organic interlayer materials comprise a growing subject of fundamental academic research and practical development, since they allow synthetic tailoring of properties and are compatible with device fabrication approaches, such as slot-die coating, ink-jet printing, and spray-coating [30]. These interlayer materials, that modify the electrode work function, including polyelectrolytes, polymer zwitterions, and neutral fluorocarbon-, ethylene glycol-, and amine-functionalized materials, have been developed for OLEDs, OFETs and OPVs [20]. Not only can they replace the most efficient inorganic interlayer materials, but they can also lead to superior device efficiency and stability. The use of solution-processed organic inter layers in multilayered device structures is enabled by their solubility in solvents that are orthogonal to those that solubilize the organic active layers [31,32]. Although the electronic utility is derived mainly from modification of the electrode work function, these materials are notably multifunctional, with rheological, morphological, electronic, and optical properties that may all be optimized to advantage of device performance.

In this perspective, we discuss the mechanism of metal work function reduction using polymer interlayers and describe recent studies on the mechanism of surface modification based on several material systems, including CPEs, polymeric amines and CPZs. We then summarize comprehensive efforts to develop polymer modification platforms and present the understanding of multiple functionalities of these materials as cathode modification interlayers in BHJ OPVs, OLEDs and OFETs. Our intent is to bridge the knowledge and terminology gaps among materials designers, device engineers, and condensed matter physicists working in this exciting field.

2. The mechanism of work function reduction

Tremendous research efforts have been devoted to understanding the mechanisms of energy level alignment at the interface where organic semiconductors contact metal electrodes. Several semi-empirical models were proposed to describe such interfaces, including the charge-transfer model and the interfacial doping model [33–37]. However, none fully explains the experimental observations at such interfaces. So, we simply provide a discussion of the mechanisms associated with the polymer interlayers that are relevant for the following sections. For example, conjugated polyelectrolytes (CPEs), the widely used surface modifiers in OEs, show thickness dependent effects on metal work function modification. Specifically, in the case of very thin (< 10 nm) polyelectrolyte interlayers, Lee et al. proposed that the generation of permanent interfacial dipoles on the metal electrode is the dominant mechanism for CPE tuning of metal work function (Fig. 1A, B). However, when the interlayer thickness exceeds the quantum mechanical tunneling limit (~10 nm), one has to consider the effect of counter ion migration and molecular reorientation (Fig. 1C). Under an external electric field, the counter ions of CPEs may migrate to the respective electrodes, while the ionic pendant groups of CPEs orient adjacent to the electrodes. Thus, the mobile counter ions in CPEs play a critical role on surface electronic modification of the metal [38]. Interestingly, different ionic groups of the CPEs will influence interfacial dipole generation and orientation, inducing various degrees and direction of vacuum energy level shifting [39]. Hence, the polyelectrolyte surface modifier generally enables metal work function reduction by forming net dipoles at the organic/electrode interface.

Amine functionalized polymers were also found to reduce metal work function efficiently. Insightful reports by Zhou et al. [40] showed that the work function reduction by the amine groups

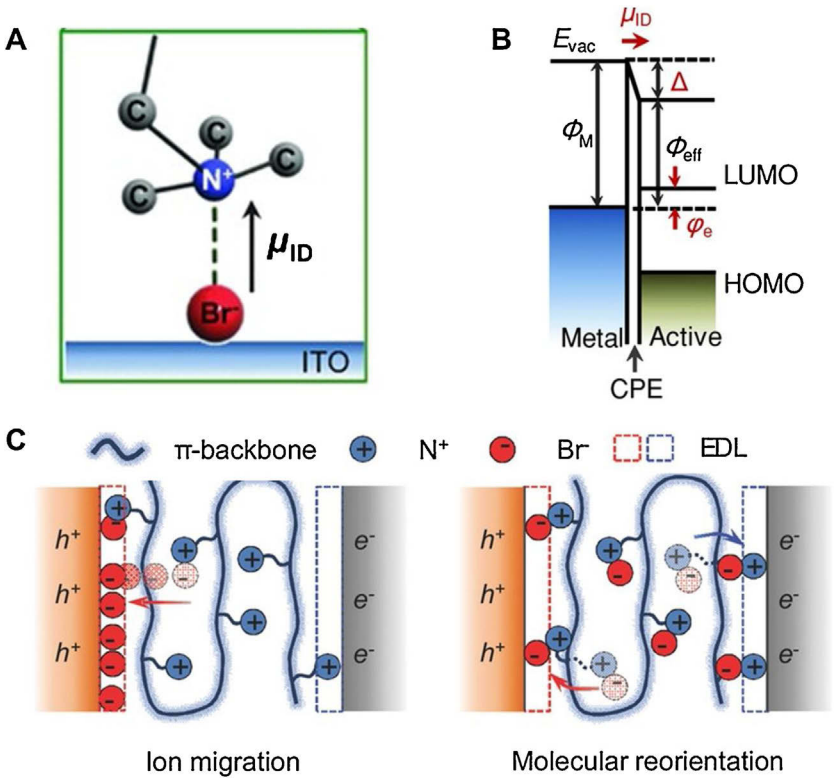

Fig. 1. (A) Interfacial dipole induced by ionic groups, such as ammonium bromides, in CPEs; (B) schematic energy level diagram of the metal/CPE/active layer in OE devices; (C) schematics of the working mechanism of thick CPEs (>10 nm) under bias. [38], Copyright 2014. Reproduced with permission from John Wiley and Sons Inc.

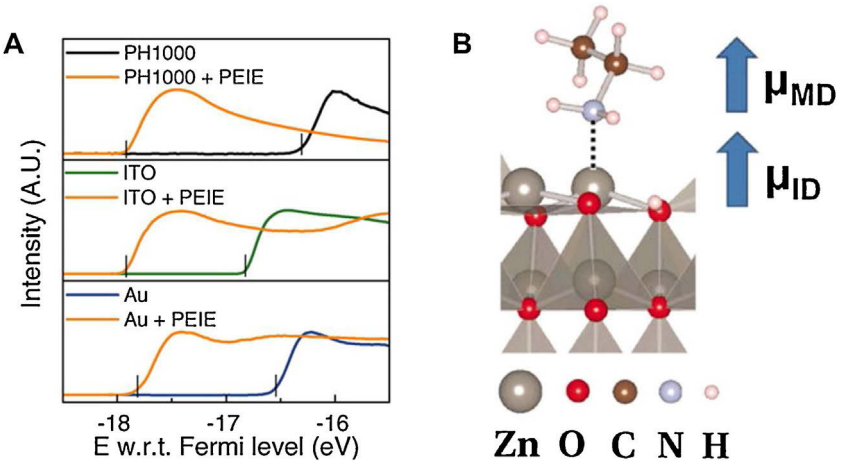

Fig. 2. (A) Secondary electron cut-off obtained *via* UPS for PEDOT: PSS (PH1000), ITO, and Au compositions, with and without PEIE interlayers, showing the general work function reduction of different conductive electrodes resulting from PEIE modification; (B) scheme of molecular dipole or interfacial dipole generated by PEI/PEIE on a zinc oxide surface. [40], Copyright 2012. Reproduced with permission from the American Association for the Advancement of Science.

in PEIE is nearly equivalent on different electrodes (Fig. 2A). The mechanism of this effect is attributed to both the orientation of the internal molecular dipole that is induced by the electron pair on the nitrogen atom, and an interfacial dipole that is due to the partial charge transfer from the amine groups to the metal upon physical adsorption (Fig. 2B). When the amine groups are connected covalently to electroactive components, such as fullerenes, the resultant interlayer materials exhibit a work function "pinning effect", with ability to reduce the work function of numerous metal electrodes to the same level [31]. Thus, amine-containing interlayers show a general effect towards reducing work function across metal compositions.

In contract to polyelectrolytes, polymer zwitterions are neutral, hydrophilic surface modifiers. The pendent zwitterions, while uncharged, can be viewed as side chain dipole moments that impart an electronic influence on their surroundings and provide an excellent model to understand the effect of dipole orientation on surface modification without the complication of counter ion migration (Fig. 3A). For example, sulfobetaine (SB) zwitterions have a calculated permanent dipole moment of 15.2 Debye [41], in which the negative charge is distributed predominantly on the sulfonate and the positive charge on the ammonium. A classical electrostatic model of an image dipole interaction was proposed to describe the mechanism of zwitterion/metal interactions [42]. Consider an electrostatic dipole $\boldsymbol{p_o}$ near a metal surface at a distance $\boldsymbol{r}$ (Fig. 3B).

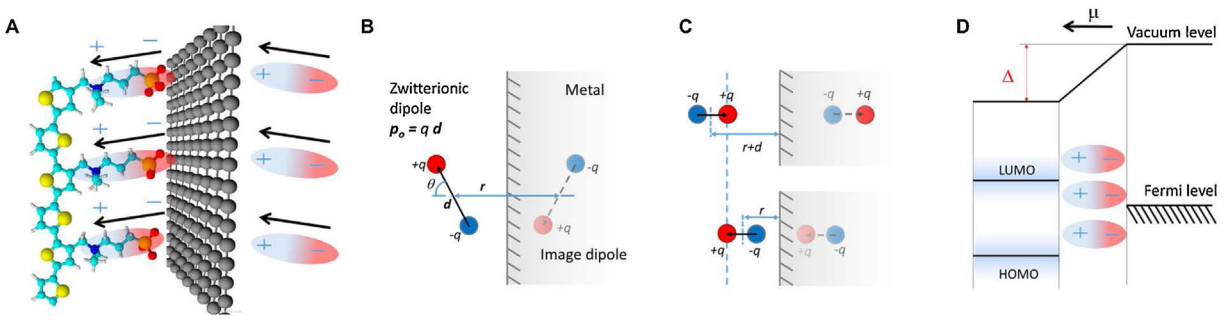

Fig. 3. (A) Schematic depiction of SB zwitterions as pendent groups on a polymer backbone near a metal surface; (B, C) depiction of an image dipole where the original dipole $\boldsymbol{p_o} = q\boldsymbol{d}$ (q is the elementary charge, $\boldsymbol{d}$ is a vector pointing from a negative charge, $-q$, to a positive charge, $+q$) located at a distance $\boldsymbol{r}$ from a metal surface; (D) net dipole alignment on a metal surface creates an interfacial dipole (Δ). [44], Copyright 2016. Reproduced with permission from the American Chemical Society.

Such a dipole induces surface polarization that can be described by an image charge model [42]. The positive and negative charges of the dipole would be mirrored across the plane of the metal surface by charges of identical value and opposite sign, creating an image dipole, $\boldsymbol{p_i}$. In the case of SB-functionalized polymers, negative charges on the sulfonate are located at a greater distance from the polymer backbone than the positive charges on the nitrogen. Hence, the former is more susceptible to reorientation under an applied electric field, while the latter is relatively fixed. If the dipole is fixed at a point of positive charge, the torque $\boldsymbol{\tau}$, given by (Eq. 1), will cause the original dipole to rotate.

$$\boldsymbol{\tau} = \left[\boldsymbol{p}_0 \times \boldsymbol{E_{dip-dip}}\right] = \frac{1}{4\pi\varepsilon_0}\left[\boldsymbol{p}_0 \times \left(\frac{3\,(\boldsymbol{p_i}\cdot\boldsymbol{r})\cdot\boldsymbol{r}}{r^5} - \frac{\boldsymbol{p_i}}{r^3}\right)\right] \quad (1)$$

In principle, two quasi-stable orientations that are normal to the surface at $\theta = 0$ or $\theta = \pi$ are possible, i.e. with the dipole pointing away from or towards the surface (Fig. 3C). However, dipole orientation away from the surface (Fig. 3C, bottom) has a shorter distance, making this configuration energetically more favorable (Fig. 3C, top) as can be seen from the interaction energy given by Eq. 2.

$$U_{dip-dip} = \frac{1}{8\pi\varepsilon_0}\left(\frac{\boldsymbol{p_o}\cdot\boldsymbol{p_i}}{r^3} - \frac{3\,(\boldsymbol{p_o}\cdot\boldsymbol{r})(\boldsymbol{p_i}\cdot\boldsymbol{r})}{r^5}\right) \quad (2)$$

Hence, in the vicinity of a metal surface, the self-induced torque of side chains and energy minimization will direct the negative charges of the sulfonate towards the metal surface (Fig. 3A). Such a net charge redistribution creates an interfacial dipole (Δ) at the metal-polymer zwitterion interface (Fig. 3D), i.e. giving a lower work function of the polymer/metal system which represent the electrode. Some experimental results also support the preferential orientation of SB zwitterions on the metal surface as assumed in the classical electrostatic model. For example, studies of DeLongchamp and coworkers revealed a net perpendicular orientation of SB side chains on Au and ITO substrates using the carbon K-edge of NEXAFS measurements [41,43]. Moreover, Richter and coworkers employed VR-SFG measurements to acquire structural information of the -SO_3^- group in zwitterion-substituted polymers and fullerenes on Au and ITO substrates. The VR-SFG spectrum indicated a net orientation of – C–SO_3^- throughout the entire film with the -SO_3^- groups directed towards the Au and ITO surfaces, which is consistent with the preferential orientation of zwitterionic dipoles described in the theoretic treatment [41,43].

3. Conjugated polymer interlayers

3.1. Conjugated polyelectrolytes (CPEs)

CPEs are polymers comprised of a π-conjugated backbone with pendant side chains bearing ionic functional groups (Fig. 4). Numerous polyfluorene-based CPEs were found to increase the V_{OC} of solar cell devices when integrated as interlayers between the active layer and metal cathode [26]. Subsequently, polythiophene-based CPEs were developed as cathode interlayers to improve the efficiency of polymer solar cells containing a typical photoactive layer of PCDTBT: $PC_{71}BM$ [45]. Notably, the CPEs containing polythiophene backbones showed a HOMO energy level of ~5 eV [46], close to the work function of PEDOT:PSS, and the HOMO energy level of PCDTBT (~5.5 eV) in the active layer. Thus, an ultrathin interlayer, below the quantum mechanical tunneling limit (~10 nm), is needed to achieve device performance. When these polythiophene-based CPEs were combined with electron-collecting Al electrodes, the electron extraction process of the devices improved significantly, yielding higher PCE values. Polythiophene-based CPE (P3TMAHT) interlayers have been shown to increase the V_{OC} of the devices, from 0.82 ± 0.01 V (control devices without interlayers) to 0.89 ± 0.01 V (with interlayers). The J_{SC} and *FF* of the devices also improved when polythiophene-based CPE interlayers were present, which increased PCE from 5.3 % to 6.5 % [45]. Further studies showed that introducing hydrophobic polyfluorene segments into the polythiophene-based CPE promoted self-assembly of the resultant polymer (PF2/6-*b*-P3TMAHT) into two-dimensional layered aggregates. However, PF2/6-*b*-P3TMAHT still provided a polar surface when coated on top of the active layer and the resultant self-assembled structures had negligible impact on the generation of interfacial dipoles, yielding similar device characteristics as the thiophene-based homopolymer (P3TMAHT) [45]. Another polyfluorene-based interlayer, WPF-6-oxy-F, was synthesized by Kim and coworkers [47], has ethylene oxide side groups on the fluorene unit, which induce large interfacial dipoles between the active layer and metal electrode. The OPV device with a configuration of ITO/PEDOT: PSS/P3HT:$PC_{71}BM$/ WPF-6-oxy-F(3 nm)/Al exhibits a PCE of 3.89 %, which is higher than the PCE of the device without the interlayer (2.30 %). The large PCE improvement is mainly due to the V_{OC} increase from 0.53 V to 0.64 V, arising from the interfacial dipole between the active layer and Al. In addition, WPF-6-oxy-F can also be used as an interlayer between multilayer graphene and a P3HT:$PC_{71}BM$ active layer. The PCE of this OPV device is 1.23 % with a configuration of multilayer graphene/ WPF-6-oxy-F/ P3HT:$PC_{71}BM$/PEDOT: PSS/Al. In contrast, no PCE was obtained for the devices without WPF-6-oxy-F, suggesting the ability of WPF-6-oxy-F to transport electrons from the active layer to Al [48]. CPEs were also widely investigated to promote the electron injection process of OLED devices. For example, Cao and coworkers studied polyfluorene-based CPEs in OLEDs with a device configuration of ITO/PEDOT: PSS/MEH-PPV/CPEs (3–20 nm thick)/Al [49]. The insertion of PF-NR_3^+ Br^- or PF-NR_3^+ I^- as an interlayer between the metal electrode (Al) and semiconductor layer efficiently promoted electron injection into the electroluminescent layer (MEH-PPV), affording high performance OLEDs, comparable to devices using

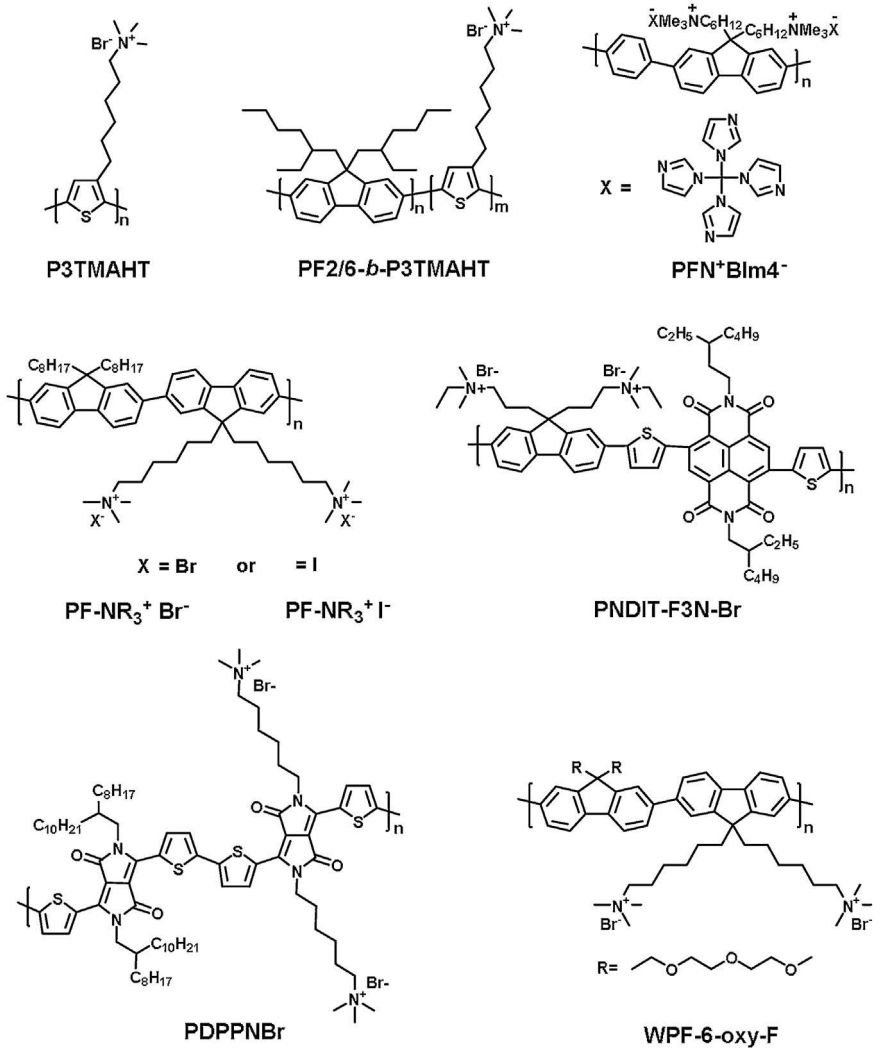

Fig. 4. Chemical structures of some representative CPEs.

low work function cathodes (Ca/Al or Ba/Al). The generation of interfacial dipoles at the CPE/Al interface that break the electron injection barrier is the main contributor to the enhanced efficiency. Along similar lines, some other polyfluorene-based CPEs were also developed to improve OLED performance [28]. Interestingly, Bazan and coworkers found the response time of OLED devices containing CPEs was strongly dependent on the applied voltage. The conjugated backbone, charged pendant groups, and counter ions in CPEs were also examined as means to optimize their performance [50,51]. Due to the combination of ionic and electronic conduction mechanisms, devices containing $PFN^{+}BIm_{4}^{-}$ interlayers showed a slow response time. Further studies showed that the response time of the devices was related to interlayer thickness and specifically that a thinner interlayer afforded a faster response. Later, Bazan and coworkers found that CPE interlayers decrease the contact resistance between a stable high work function metal electrode and an organic semiconductor, thus improving electron mobility of thin film transistors. It was proposed that the aligned interfacial dipole layer generated by the CPE interlayers caused a downward shift in the vacuum level at the interface, which decreased the electron injection energy barrier in the area of contact between the metal electrodes and organic semiconductors [52]. Most recently, low band gap CPEs were developed as interlayers in OPVs [53,54], such as CPEs containing DPP or NDI units (PDPPNBr, PNDIT-F3N-Br) [55]. PDPPNBr showed high electron mobility and conductivity due to the electron deficient and planar polymer backbone, affording better device performance as cathode interlayers when compared to the inorganic zinc oxide counterpart. Combining NDI and fluorene to afford the resultant polymer (PNDIT-F3N-Br) with more π-delocalized planar conjugated backbone promoted electron mobility while the ammonium side chains affected interfacial modification. Interestingly, PNDIT-F3N-Br showed a self-doping effect and ability to dope $PC_{71}BM$ in the photoactive layer, as revealed by ESR measurements. Overall, the power of PNDIT-F3N-Br on electron transport and interfacial modification significantly improved the solar cell efficiency, demonstrating great promise of CPEs with n-type backbones as interlayers in OEs.

3.2. Conjugated polymer zwitterions (CPZs)

CPZs contain a conjugated polymer backbone and zwitterionic side chains, making them neutral, hydrophilic, polymer semiconductors. The pendent zwitterions allow the polymers to be dissolved and processed in alcohol-based solvents and open the door for using these materials as interfacial components of optoelectronic devices [44]. Fang et al. [56] and Duan et al. [57] found that zwitterionic polyfluorene derivatives when used as electron injection layers of OLEDs improved the response time of the devices, due to the absence of counter-ions. Later improve-

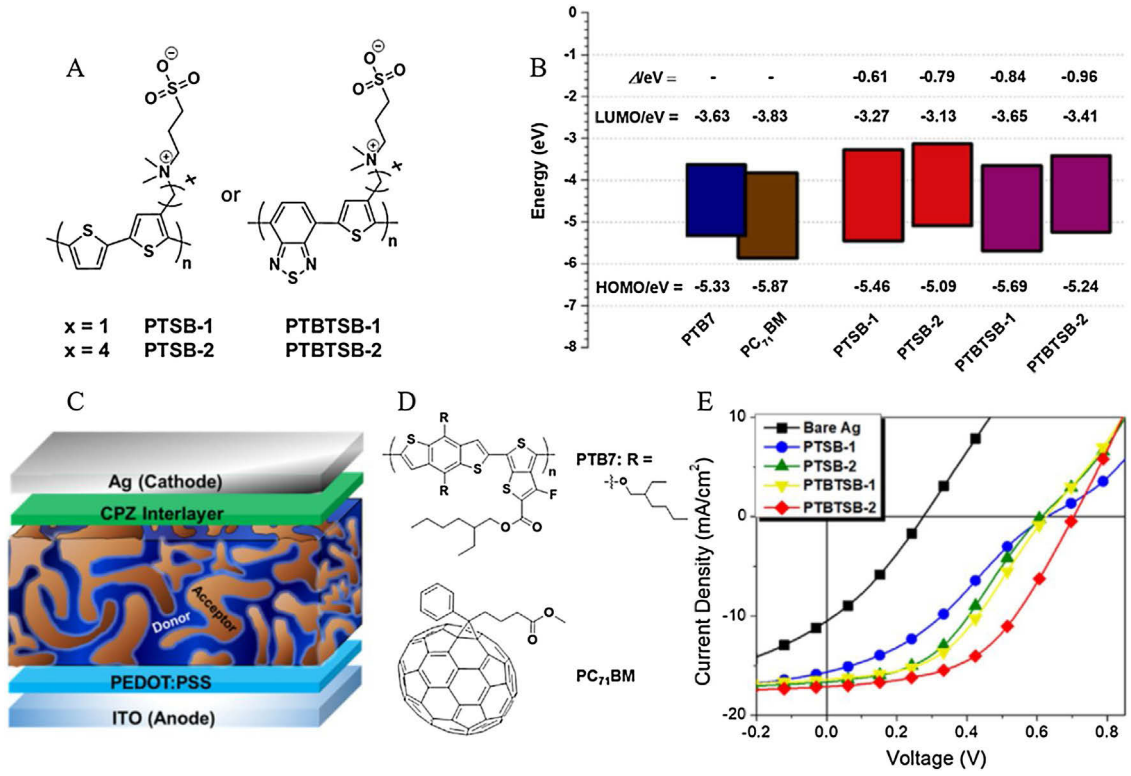

Fig. 5. (A) Chemical structures of CPZs; (B) energy levels of PTB7, $PC_{71}BM$, and CPZs (interfacial dipole (Δ) were measured on Ag); (C) solar cell device structure containing CPZ interlayers; (D) chemical structure of PTB7 and $PC_{71}BM$; (E) the corresponding device performance. [44] with a PTB7: $PC_{71}BM$ photoactive layer. Copyright 2016. Reproduced with permission from the American Chemical Society.

ments of these polyfluorenes, by post-polymerization chemistry, enhanced their use as interlayers to improve electron extraction in OPVs [58]. Emrick and coworkers developed strategies for synthesizing numerous zwitterion-containing aromatic monomers and conditions for their polymerization. These CPZs were designed and synthesized as interfacial materials for OPVs [44]. For example, polythiophene-based CPZs were synthesized and integrated into OPV devices as cathode interlayers (Fig. 5) [42,59]. For devices containing Ag cathodes, the interlayes improved device efficiency by inducing a large interfacial dipole (Δ) that reduced the work function of silver, affording a higher V_{bi} in the fabricated devices. It was shown that CPZ copolymers with benzothiadiazole units, PTBTSB-1 and PTBTSB-2, can generate even larger interfacial dipole (Δ) values on silver electrodes. Interestingly, polymers containing longer side chains (PTSB-2, PTBTSB-2) induced the highest interfacial dipole (Δ) values, most likely due to better side chain flexibility that provides more freedom for molecular reorientation along the surface normal of the metal electrodes. This is in good agreement with the larger V_{OC} in OPVs that was achieved by PTBTSB-2 as the interlayer. In consideration of the energy levels of the photoactive layers used in the devices, one would expect that the deeper HOMO and LUMO energy levels of PTBTSB-1 would provide better electron extraction and hole blocking properties at the interface yielding devices with high J_{SC} and *FF*. However, PTBTSB-2, with higher HOMO and LUMO levels, afforded devices with even higher J_{SC} and *FF*, indicating that higher V_{bi}, as determined by larger interfacial dipole (Δ), is most crucial for enhancing J_{SC} and *FF*. Similar results were also found by Duan et al. who reported that zwitterionic polyfluorene interlayers with different energy levels can afford devices with different V_{bi} and thus tunable solar cell performance [58].

Conjugated polymers with D-A backbones are advantageous due to their easily tunable energy levels. For example, CPZ interlayer materials containing DPP or *i*In backbones (Fig. 6) improved OPV performance significantly relative to control devices [60]. Distinct from the polythiophene-based CPZs, the DPP- or *i*In- based CPZs show a quite similar effect on reducing the metal work function with no apparent backbone dependence. However, the polymer backbone chemistry does play a critical role in dictating the HOMO and LUMO energy levels of the CPZ interlayers, which impacts electrons extraction and hole blocking from the active layer. Specifically, studies on *i*In-based CPZs indicate that a relatively deep LUMO level is crucial for promoting electron extraction. Additionally, in DPP-based CPZs, PT_3DPPSB and PT_2BTDPPSB show similar HOMO levels. Thus, the deeper LUMO level of PT_2BTDPPSB drives higher *FF* and J_{SC} values in solar cells. Conjugated backbones also have a crucial effect on charge transport of the interlayer materials [61,62]. The electron mobility of the interlayer materials significantly improved when going from PT_3SB to PT_2BTDPPSB to PT_2NDISB, as evidenced by SCLC measurements. CPZs having the typical p-type polythiophene backbones (PT_3SB) show poor electron transport properties ($\mu_e = 1 \times 10^{-8}$ cm^2/Vs), thus for devices containing PT_3SB it is impossible to obtain maximum V_{OC}, J_{SC} and *FF* values at the same interlayer thickness, since the thicker interlayer (> 7 nm) has a higher V_{OC} at the expense of dramatically decreased J_{SC} and *FF* (Fig. 7A, B). PT_2NDISB with the classical n-type backbone has proven to be a successful interlayer design, showing the highest electron mobility (2×10^{-6} cm^2/Vs) and affording some of the best performing CPZ-containing solar cells to date. The efficient charge transport, combined with the much deeper HOMO and LUMO levels of PT_2NDISB, contribute to its superior performance. PT_2BTDPPSB shows an electron mobility of 2×10^{-7} cm^2/Vs, one order of magnitude lower than PT_2NDISB, but still affords a device performance comparable to PT_2NDISB-based devices. This suggests that the narrow E_g, large interfacial dipole (Δ), and sufficiently low LUMO level of PT_2BTDPPSB combine to generate excellent performance as a cathode interlayer, or the electron mobility is high enough to provide efficient electron transport across the thin interlayer. Because of their relatively high electron mobility,

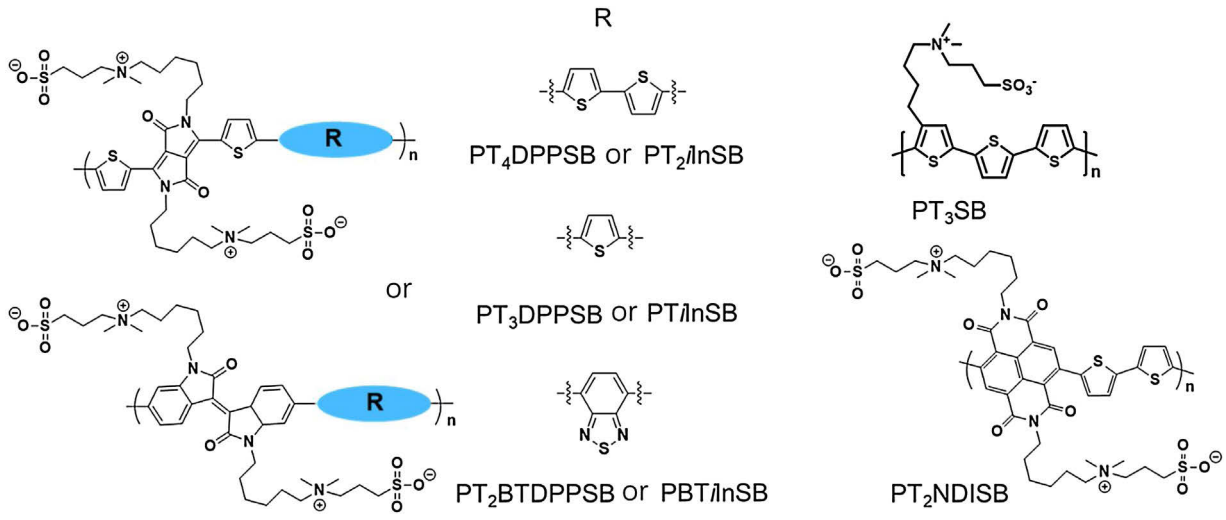

Fig. 6. Chemical structures of some typical CPZs.

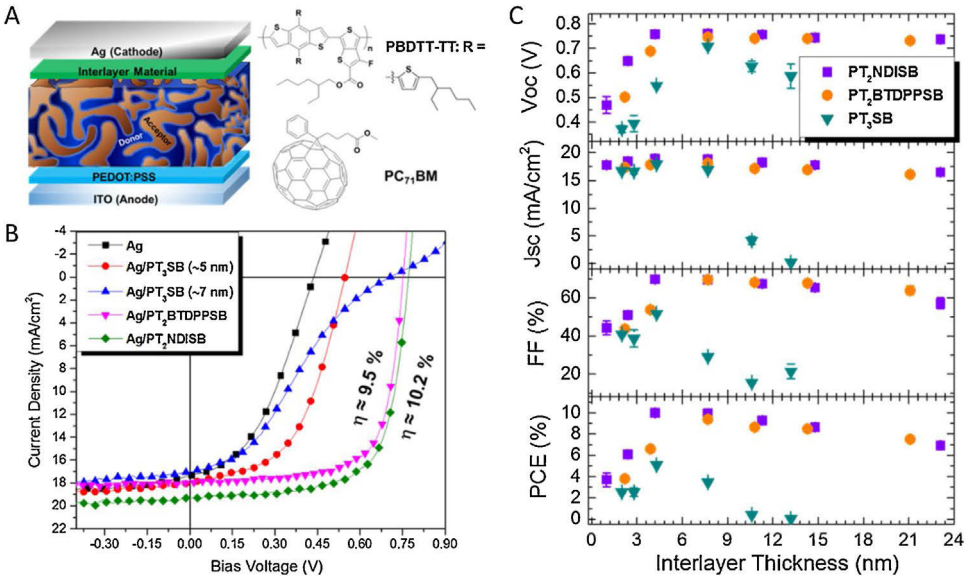

Fig. 7. (A) Solar cell structure and the active layer materials (PBDTT-TT: $PC_{71}BM$) used for evaluating interlayer materials; (B) current density-voltage curves of the solar cell devices containing different CPZ interlayers; (C) solar cell device performance *vs.* different CPZ interlayer thickness. [44], Copyright 2016. Reproduced with permission from the American Chemical Society.

both PT_2NDISB and PT_2BTDPPSB are more tolerant of interlayer thickness variations, with V_{OC} and *FF* plateauing at 5–10 nm, but keeping approximate maximum values for thicknesses greater than 20 nm (Fig. 7C). These results indicate that it is crucial to optimize the electron transport and LUMO energy level of the cathode interlayers to suppress charge accumulation at the photoactive layer/electrode interface. In addition, high performance interfacial materials should be suitable for facile and large area processing, while circumventing the need for precise nanoscale thickness control to achieve high device performance.

3.3. Neutral conjugated polymers

In comparison to polyelectrolytes, neutral polymers have relatively simple structures that lack any potential complications associated with mobile counterions. Numerous neutral conjugated polymers have been designed and synthesized to the benefit of organic electronic devices. The most representative examples are amine-functionalized polymers, especially PFN (Fig. 8) and its derivatives. PFN and its quaternized derivatives, synthesized in 2004 by Cao and coworkers, demonstrated enhanced electron injection as cathode interlayers in OLED devices [49]. Later, PFN was found to significantly improve solar cell performance when integrated as a thin buffer layer between the Al cathode and photoactive layer [63]. Further investigations showed that the work function of ITO was decreased from 4.7 to 4.1 eV with an ultrathin PFN film (10 nm), affording Ohmic contact between the photoactive layer and ITO electrode in inverted OPVs. PFN is more efficient as an ITO modifier to support the fabrication of inverted OPVs with high efficiencies, as demonstrated by He and others [64,65]. Inspired by the success of PFN, a series of neutral conjugated polymer interlayers were developed and successfully applied in both OLEDs and OPVs, such as amino N-oxides and phosphonate-functionalized polyfluorene (PFN-OH, PF-EP) [23]. Similar to PFN, PFN-OH improves electron injection from high work function metal cathodes to active layers, affording high performance OLEDs. Zhou et al. found that PF-EP can be used to fabricate blue OLEDs, as both a light-emitting and electron injection material, due to the interaction between the

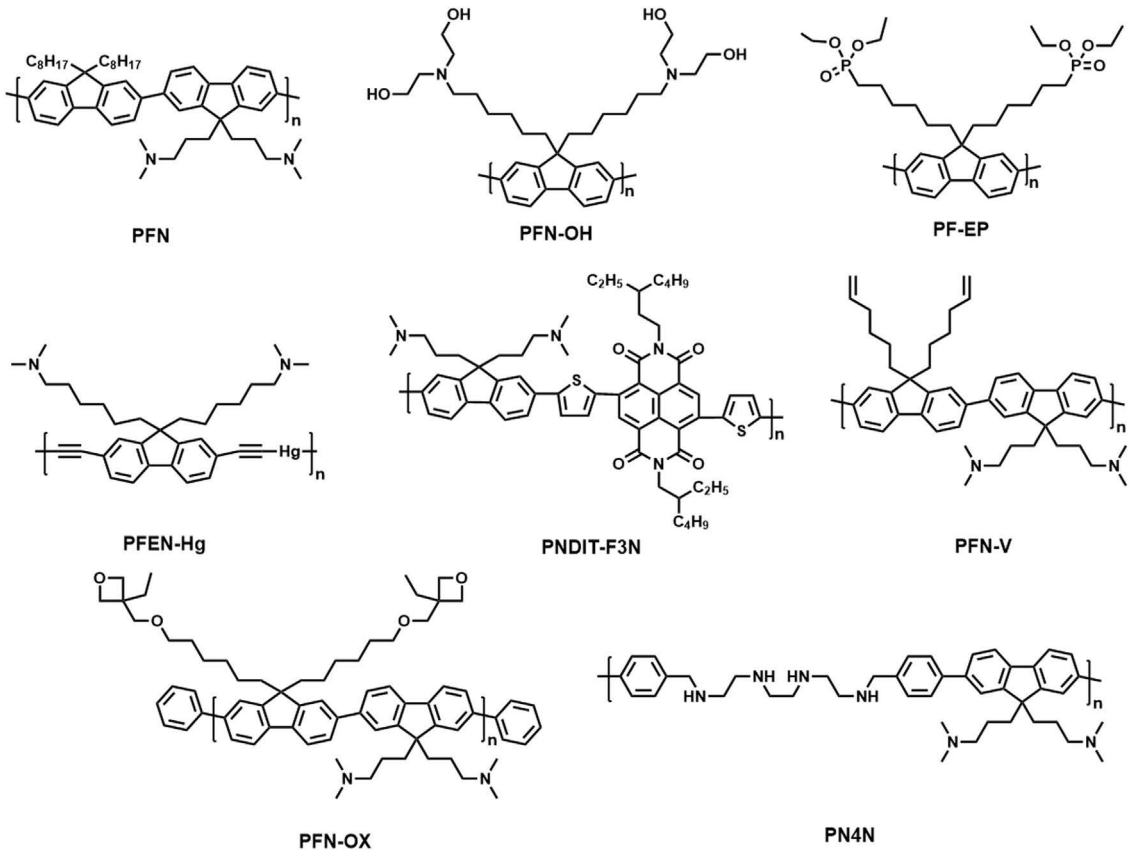

Fig. 8. Chemical structures of some neutral conjugated polymers.

phosphonate groups and the Al cathode [66]. The OLED device performance, when using such interlayers is comparable to, or greater than those devices using Ca or Ba cathodes. Later, polymer interlayers with phosphonate functionalities were also found to efficiently decrease the ITO work function, holding great potential to facilitate electron extraction from the active layer to ITO for inverted OPVs [67]. Due to the low intrinsic conductivity of PFN, the working thickness of PFN interlayers for device applications is usually restricted to less than 10 nm (the quantum mechanical tunneling limit). To develop novel interlayer materials suitable for facile processing and lacking stringent thickness requirements, extensive research has been devoted to modifying the PFN backbone. For example, Cao and coworkers designed and synthesized Hg-containing derivative of amino-functionalized conjugated polymers (PFEN-Hg) [68], a metallopolymer that showed orthogonal solvent processability and good film formation, supporting the construction of multilayer devices *via* all-solution processes. Similar to PFN, the amino-functionalized side chains in PFEN-Hg produce the desired dipole with the ITO substrate, affording efficient electron extraction in inverted OPVs. Most importantly, the noncovalent Hg–Hg interactions enhanced stacking of polymer chains, improved the charge transport and conductivity, and provided excellent performance as OPV interlayers. Later, the same group introduced NDI units into the PFN backbone to realize an n-type conjugated polymer interlayer (PNDIT-F3N) [55]. Interestingly, PNDIT-F3N showed a photo-induced conductivity enhancement, affording efficient OPV devices as thickness-insensitive cathode interlayers. Recently, a cross-linkable conjugated polymer interlayer, PFN-V, was reported by Wang et al [69]. PFN-V can react with 1,8-octanedithiol *via* "click" chemistry, which will increase the thermal and morphological stability of the interlayers. The crosslinked PFN-V films show strong solvent resistance and modify the ITO electrode efficiently, affording Ohmic contact between the ITO cathode and active layer. The surface energy of the crosslinked PFN-V film also promotes a favorable vertical phase separation of the bulk heterojunction active layer, further enhancing the OPV device performance. The doping effect is important for neutral polymers, due to increasing carrier concentration and enhancing charge transport. There are two water/alcohol soluble conjugated polymer interlayers with polyfluorene backbones exhibiting enhanced device performance when blended with other components. PFN-OX is a cross-linkable n-type polymer interlayer synthesized by Cao and coworkers. [36] Inverted OPV devices were fabricated with a configuration of ITO/ZnO/PFN-OX/PTB7:$PC_{71}BM$/MoO_3/Al. The device with PFN-OX achieved 9.28 % PCE, an improvement over devices without PFN-OX (8.45 %). PFN-OX not only tunes the work function of the cathode to increase the V_{OC} but also dopes $PC_{71}BM$ to promote electron extraction. OFET devices were also fabricated by using PFN-OX as an interlayer to understand the electron extraction and hole blocking function. The device with PFN-OX showed an enhanced current in the forward direction and a reduction in the reverse direction in the dark. The insertion of PFN-OX at the electrode/organic semiconductor interface also decreased the I_{ds} of the p-channel OFET. These two phenomena confirm the desired function of both electron extraction and hole blocking by PFN-OX. Cao and coworkers also reported a polymer interlayer termed PN4N, which can play a role as an amino-functionalized polymer dopant [37]. When PN4N was blended with N2200 and a crosslinker bisPFPA, the electron mobility of the blend film increased due to the doping effect. The device performance with the doping interlayer achieved 9.94 % efficiency in comparison to the reference device with a PN4N interlayer (9.16 %). Interestingly, the interlayer can absorb light and contribute to the J_{SC} of the devices containing N2200.

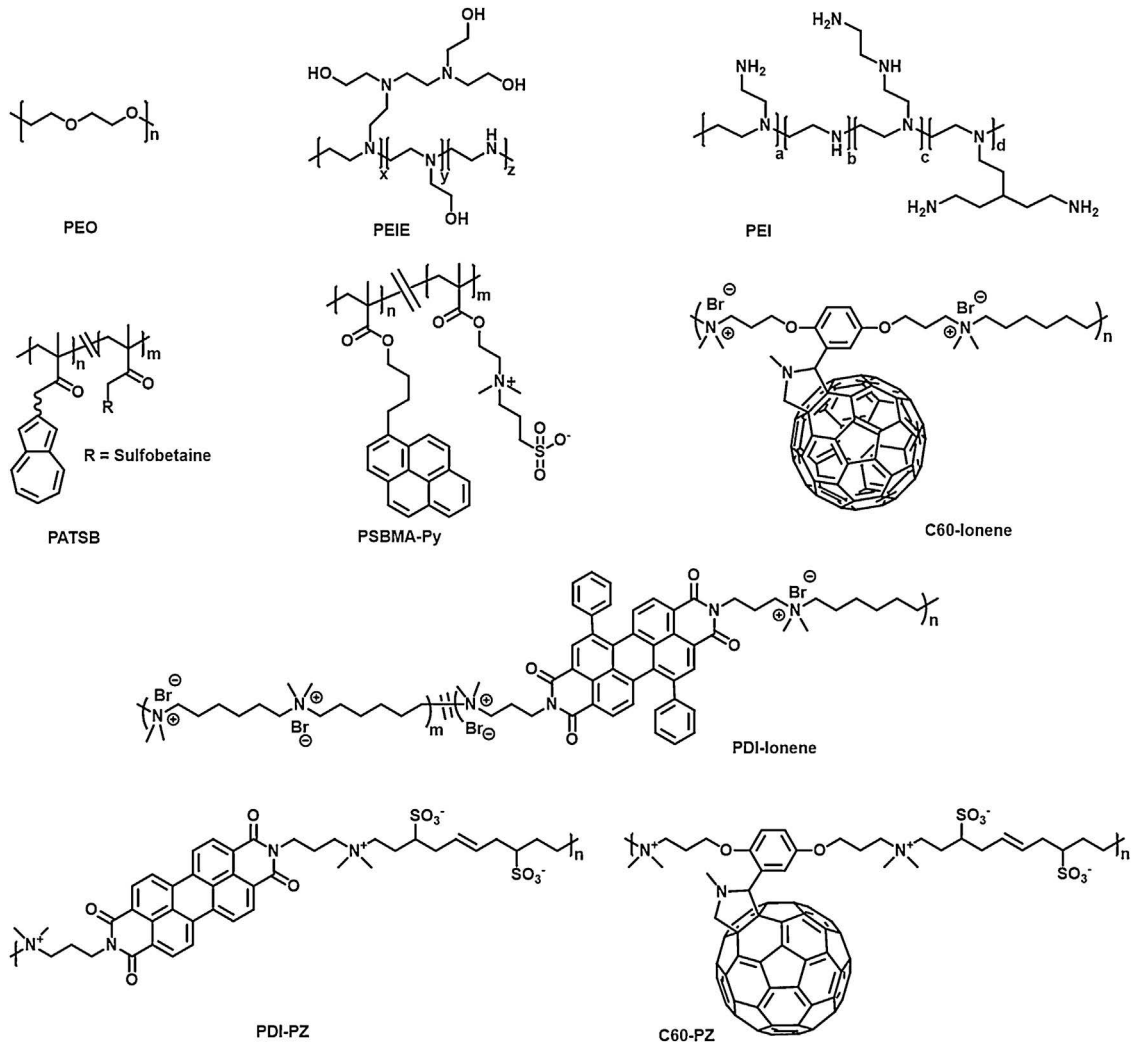

Fig. 9. Chemical structures of some representative non-conjugated polymer interlayer materials.

4. Non-conjugated polymer interlayers

Polyethylene oxide (PEO, Fig. 9) represents the first studied example of a non-conjugated polymer for ITO modification of inverted OSCs. A thin layer of PEO reduced the work function of ITO by up to 0.5 eV as indicated by UPS, promoting electron extraction from the photoactive layer [70]. Later, aliphatic amine-containing polymer interlayers, PEI and PEIE (Fig. 9), were demonstrated to universally reduce the work function of numerous conductive electrodes including metals, metal oxides, conducting polymers, graphene, and ITO by ~1 eV. It has been shown that physical adsorption of the polymers onto the electrode surface contributes to this work function reduction, independent of the surface chemistry. This low work function surface shows good air stability and can be obtained by simple solution processing methods, such as spin coating, printing, or immersing the conductors in the polymer solution [40]. The PEI or PEIE modified electrodes are now widely used in optoelectronic devices. Park et al. designed a series of polyelectrolytes containing an ethoxylated polyethyleneimine backbone with various counter ions, including Cl^-, Br^-, and I^-. These polymers reduce φ_e of OFETs, consistent with interfacial dipole or n-type doping at the electrode/semiconductor interface [71]. Thus, a controllable interfacial doping of organic semiconductors can be achieved by coating a thin layer of the polyelectrolyte. Some non-conjugated block copolymers were also found to efficiently reduce the work function of metal electrodes. For example, Emrick and coworkers synthesized novel methacrylate copolymers containing azulene (PATSB) or pyrene (PSBMA-Py) comonomers by free radical polymerization [72]. Polymer with zwitterionic substitutions (sulfobetaine) removed S-shaped kinks in the *J–V* curves of OPV devices, boosting solar cell efficiency. In simple electron-only devices, some of the non-conjugated polymer zwitterions also enhanced charge injection efficiency, showing promising applications for numerous types of electronic devices requiring a low work function electrode [41,72]. Recently, Park et al. reported a series of novel poly(ionic liquid) based block copolymers for improving performance of inverted OSCs. The electrode work function can be controlled by interfacial dipoles induced by the ionic pendent groups. Interestingly, the ionic group density plays a critical role on metal work function reduction, which can be easily tuned by simply changing the molar ratio of the imidazolium poly(ionic liquid) [73]. To overcome the inefficiency of non-conjugated polymers on charge transport, planar electronically active PDI-based units can be incorporated with polyelectrolyte dopants, as seen in the PDI-based ionene polymers (PDI-ionene). These polymers show self-doping properties, enabling chemical and morphological control of interfacial doping and charge transport. Insertion of a suitable PDI-ionene polymer as the cathode interlayer can significantly enhance the performance of both fullerene and non-fullerene based OPVs [74,75]. Very recently, we further integrated C_{60} fullerene monomers directly

into ionene polymers. The novel "C_{60}-ionene" for interface modification enables the use of numerous high work-function metals (e.g., silver, copper, and gold) as the cathode for efficient OPVs. Introducing fullerene moieties into ionene polymers dramatically improved their conductivity and afforded devices with high efficiency by reducing charge accumulation at the cathode/active layer interface [76]. A novel synthetic strategy that improves charge transport characteristics of non-conjugated polymer zwitterions was also proposed by our group. Polymer zwitterions were synthesized by the nucleophilic ring-opening of the bis-sultone, 3,3′-(but-2-ene-1,4-diyl)bis(1,2-oxathiolane 2,2-dioxide) with functional PDI or fullerene monomers. The PDI and fullerene units dictated the charge transport properties of the interlayers such that the PDI-PZ and C_{60}-PZ interlayers could overcome energy barriers at the hard-soft materials interface of OEs to the benefit of electron injection and extraction processes between metal electrodes and organic semiconductors [77].

5. Summary and outlook

Utilization of organic materials in electronic and optoelectronic devices promises to broaden the range of device applications due to low-cost, high-throughput, large-area fabrication of lightweight and mechanically flexible device architectures. However, to take advantage of the unique properties of organic semiconductors, the scalability and compatibility of device fabrication steps require further improvement. Replacement of inorganic interlayers that require vacuum-based deposition or high-temperature annealing with solution-processible organic/polymer materials has recently emerged as a successful strategy. The polymer interlayers carry numerous advantages including solution processing and robust film formation. In this contribution we surveyed recent progress on polymers for designing low work function surfaces in organic electronic devices. Despite the impresive progress achieved to works with polymer interlayers, much work lies ahead to gain more comprehensive understanding, resolve outstanding problems, and determine future directions.

First, the organic interlayers that have been developed for modifying metal work functions generally contain some unique functional groups (amine, zwitterions, electrolytes, etc.). Some of these functionalities can react with the components in the active layers. For example, recently developed non-fullerene acceptors in OPVs are chemically reactive and potentially react with some polymer interlayers, such as PEIE, causing device degradation [78]. Thus, more emphasis on chemical stability at the interface is required.

Second, the morphological stability of the polymer interlayer during device operation is complicated and not fully understood. Interlayer materials can diffuse into the active layer and cause degradation of one or both layers. The well-developed polymer interlayers are generally hydrophilic, while the active layers are usually hydrophobic. Thus, de-wetting of the polymer interlayer on the active layer can limit device performance and prevent achieving long term stability [79].

Third, the exploitation of the intrinsic chemical stability and photostability of polymer interlayers, such as interactions with air or water, and photochemical reactions within polymer interlayer or with the active layer presents an important task for future research.

Finally, various models were proposed to explain the mechanisms of energy level alignment in the area of contact between the polymer interlayer and metal electrode. However, no single model can explain all of the observed experimental results. Thus, more effort is required to understand this heterojunction interface. For example, the development of more powerful characterization techniques would benefit the understanding of the relationship between interfacial morphology and electronic structures at device interfaces, including the impact of molecular orientation and dipole orientation on energy level alignment at interfaces.

CRediT authorship contribution statement

Yao Wu: Writing - original draft. **Yao Liu:** Supervision, Conceptualization, Writing - original draft. **Todd Emrick:** Supervision, Writing - review & editing. **Thomas P. Russell:** Supervision, Writing - review & editing.

Declaration of Competing Interest

The authors declare that they have no known competing financial interests or personal relationships that could have appeared to influence the work reported in this paper.

Acknowledgements

Y.L. acknowledges the support from the National Natural Science Foundation of China (NSFC) (21875018). Y.W. and T.P.R. were supported by the Office of Naval Research, Materials Division, under contract N00014-17-1-2241. T.E. acknowledges the support from the National Science Foundation (NSF-CHE-1904660).

References

[1] Wang C, Dong H, Hu W, Liu Y, Zhu D. Semiconducting pi-conjugated systems in field-effect transistors: a material odyssey of organic electronics. Chem Rev 2012;112:2208–67.
[2] Huang Y, Kramer EJ, Heeger AJ, Bazan GC. Bulk heterojunction solar cells: morphology and performance relationships. Chem Rev 2014;114:7006–43.
[3] Lu L, Zheng T, Wu Q, Schneider AM, Zhao D, Yu L. Recent advances in bulk heterojunction polymer solar cells. Chem Rev 2015;115:12666–731.
[4] Dou L, Liu Y, Hong Z, Li G, Yang Y. Low-bandgap near-IR conjugated polymers/molecules for organic electronics. Chem Rev 2015;115:12633–65.
[5] Di Carlo Rasi D, Janssen RAJ. Advances in solution-processed multijunction organic solar cells. Adv Mater 2019;31, 1806499/1-27.
[6] Cheng P, Li G, Zhan X, Yang Y. Next-generation organic photovoltaics based on non-fullerene acceptors. Nat Photon 2018;12:131–42.
[7] Ye L, Zhang S, Huo L, Zhang M, Hou J. Molecular design toward highly efficient photovoltaic polymers based on two-dimensional conjugated benzodithiophene. Acc Chem Res 2014;47:1595–603.
[8] Wang J, Liu K, Ma L, Zhan X. Triarylamine: versatile platform for organic, dye-sensitized, and perovskite solar cells. Chem Rev 2016;116:14675–725.
[9] Hou J, Inganas O, Friend RH, Gao F. Organic solar cells based on non-fullerene acceptors. Nat Mater 2018;17:119–28.
[10] Yan C, Barlow S, Wang Z, Yan H, Jen AKY, Marder SR, et al. Non-fullerene acceptors for organic solar cells. Nat Rev Mater 2018;3:18003, 1-19.
[11] Wang C, Dong H, Jiang L, Hu W. Organic semiconductor crystals. Chem Soc Rev 2018;47:422–500.
[12] Dou JH, Zheng YQ, Yao ZF, Lei T, Shen X, Luo XY, et al. A cofacially stacked electron-deficient small molecule with a high electron mobility of over 10 $cm^2\ V^{-1}\ s^{-1}$ in air. Adv Mater 2015;27:8051–5.
[13] Paterson AF, Singh S, Fallon KJ, Hodsden T, Han Y, Schroeder BC, et al. Recent progress in high-mobility organic transistors: a reality check. Adv Mater 2018;30:1801079, 1-33.
[14] Jou JH, Kumar S, Agrawal A, Li TH, Sahoo S. Approaches for fabricating high efficiency organic light emitting diodes. J Mater Chem C 2015;3:2974–3002.
[15] Liu Y, Li C, Ren Z, Yan S, Bryce MR. All-organic thermally activated delayed fluorescence materials for organic light-emitting diodes. Nat Rev Mater 2018;3:18020, /1-20.
[16] Yang Z, Mao Z, Xie Z, Zhang Y, Liu S, Zhao J, et al. Recent advances in organic thermally activated delayed fluorescence materials. Chem Soc Rev 2017;46:915–1016.
[17] Cui Y, Yao H, Zhang J, Zhang T, Wang Y, Hong L, et al. Over 16% efficiency organic photovoltaic cells enabled by a chlorinated acceptor with increased open-circuit voltages. Nat Commun 2019;10:2515, 1-8.
[18] Meng L, Zhang Y, Wan X, Li C, Zhang X, Wang Y, et al. Organic and solution-processed tandem solar cells with 17.3% efficiency. Science 2018;361:1094–8.
[19] Anthony JE. Organic electronics: addressing challenges. Nat Mater 2014;13:773–5.
[20] Peng X, Hu L, Qin F, Zhou YH, Chu PK. Low work function surface modifiers for solution-processed electronics: a review. Adv Mater Interfaces 2018;5:1701404, 1-16.
[21] Chueh CC, Li CZ, Jen AKY. Recent progress and perspective in solution-processed Interfacial materials for efficient and stable polymer and organometal perovskite solar cells. Energy Environ Sci 2015;8:1160–89.

[22] Ma H, Yip HL, Huang F, Jen AKY. Interface engineering for organic electronics. Adv Funct Mater 2010;20:1371–88.
[23] Hu Z, Zhang K, Huang F, Cao Y. Water/alcohol soluble conjugated polymers for the interface engineering of highly efficient polymer light-emitting diodes and polymer solar cells. Chem Commun 2015;51:5572–85.
[24] Hu ZH, Zhong ZM, Chen YW, Sun C, Huang F, Peng JB, et al. Energy-level alignment at the organic/electrode interface in organic optoelectronic devices. Adv Funct Mater 2016;26:129–36.
[25] He Z, Wu H, Cao Y. Recent advances in polymer solar cells: realization of high device performance by incorporating water/alcohol-soluble conjugated polymers as electrode buffer layer. Adv Mater 2014;26:1006–24.
[26] Duan C, Zhang K, Zhong C, Huang F, Cao Y. Recent advances in water/alcohol-soluble pi-conjugated materials: new materials and growing applications in solar cells. Chem Soc Rev 2013;42:9071–104.
[27] Yin Z, Wei J, Zheng Q. Interfacial materials for organic solar cells: recent advances and perspectives. Adv Sci 2016;3:1500362, 1-37.
[28] Huang F, Wu H, Cao Y. Water/alcohol soluble conjugated polymers as highly efficient electron transporting/injection layer in optoelectronic devices. Chem Soc Rev 2010;39:2500–21.
[29] Graetzel M, Janssen RA, Mitzi DB, Sargent EH. Materials interface engineering for solution-processed photovoltaics. Nature 2012;488:304–12.
[30] Li D, Lai WY, Zhang YZ, Huang W. Printable transparent conductive films for flexible electronics. Adv Mater 2018;30:1704738, 1-24.
[31] Page ZA, Liu Y, Duzhko VV, Russell TP, Emrick T. Fulleropyrrolidine interlayers: tailoring electrodes to raise organic solar cell efficiency. Science 2014;346:441–4.
[32] Liu Y, Page Z, Ferdous S, Liu F, Kim P, Emrick T, et al. Dual functional zwitterionic fullerene interlayer for efficient inverted polymer solar cells. Adv Energy Mater 2015;5:1500405, 1-6.
[33] Braun S, Salaneck WR, Fahlman M. Energy-level alignment at organic/metal and organic/organic interfaces. Adv Mater 2009;21:1450–72.
[34] Bao Q, Liu X, Wang E, Fang J, Gao F, Braun S, et al. Regular energetics at conjugated electrolyte/electrode modifier for organic electronics and their implications on design rules. Adv Mater Interfaces 2015;2:1500204, 1-6.
[35] Li CZ, Chueh CC, Ding F, Yip HL, Liang PW, Li X, et al. Doping of fullerenes via anion-induced electron transfer and its implication for surfactant facilitated high performance polymer solar cells. Adv Mater 2013;25:4425–30.
[36] Zhang K, Zhong C, Liu S, Mu C, Li Z, Yan H, et al. Highly efficient inverted polymer solar cells based on a cross-linkable water-/alcohol-soluble conjugated polymer interlayer. ACS Appl Mater Interfaces 2014;6:10429–35.
[37] Dong S, Hu Z, Zhang K, Yin Q, Jiang X, Huang F, et al. Cross-linkable and dual functional hybrid polymeric electron transporting layer for high-performance inverted polymer solar cells. Adv Mater 2017;29:1701507, 1-6.
[38] Lee BH, Jung IH, Woo HY, Shim HK, Kim G, Lee K. Multi-charged conjugated polyelectrolytes as a versatile work function modifier for organic electronic devices. Adv Funct Mater 2014;24:1100–8.
[39] Kang R, Oh SH, Kim DY. Influence of the ionic functionalities of polyfluorene derivatives as a cathode interfacial layer on inverted polymer solar cells. ACS Appl Mater Interfaces 2014;6:6227–36.
[40] Zhou Y, Fuentes-Hernandez C, Shim J, Meyer J, Giordano AJ, Li H, et al. A universal method to produce low-work function electrodes for organic electronics. Science 2012;336:327–32.
[41] Lee H, Puodziukynaite E, Zhang Y, Stephenson JC, Richter LJ, Fischer DA, et al. Poly(sulfobetaine methacrylate)s as electrode modifiers for inverted organic electronics. J Am Chem Soc 2015;137:540–9.
[42] Liu F, Page ZA, Duzhko VV, Russell TP, Emrick T. Conjugated polymeric zwitterions as efficient interlayers in organic solar cells. Adv Mater 2013;25:6868–73.
[43] Lee H, Stephenson JC, Richter LJ, McNeill CR, Gann E, Thomsen L, et al. The structural origin of Electron injection enhancements with fulleropyrrolidine interlayers. Adv Mater Interfaces 2016;3:1500852, 1-7.
[44] Liu Y, Duzhko VV, Page ZA, Emrick T, Russell TP. Conjugated polymer zwitterions: efficient interlayer materials in organic electronics. Acc Chem Res 2016;49:2478–88.
[45] Seo JH, Gutacker A, Sun Y, Wu H, Huang F, Cao Y, et al. Improved high-efficiency organic solar cells via incorporation of a conjugated polyelectrolyte interlayer. J Am Chem Soc 2011;133:8416–9.
[46] Gutacker A, Adamczyk S, Helfer A, Garner LE, Evans RC, Fonseca SM, et al. All-conjugated polyelectrolyte block copolymers. J Mater Chem 2010;20:1423–30.
[47] Oh SH, Na SI, Jo J, Lim B, Vak D, Kim DY. Water-soluble polyfluorenes as an interfacial layer leading to cathode-independent high performance of organic solar cells. Adv Funct Mater 2010;20:1977–83.
[48] Jo G, Na SI, Oh SH, Lee S, Kim TS, Wang G, et al. Tuning of a graphene-electrode work function to enhance the efficiency of organic bulk heterojunction photovoltaic cells with an inverted structure. Appl Phys Lett 2010;97:213301, 1-4.
[49] Wu HB, Huang F, Mo YQ, Yang W, Wang DL, Peng JB, et al. Efficient electron injection from a bilayer cathode consisting of aluminum and alcohol-/water-soluble conjugated polymers. Adv Mater 2004;16:1826–30.
[50] Hoven C, Yang R, Garcia A, Heeger AJ, Nguyen TQ, Bazan GC. Ion motion in conjugated polyelectrolyte electron transporting layers. J Am Chem Soc 2007;129:10976–7.
[51] Hoven CV, Yang R, Garcia A, Crockett V, Heeger AJ, Bazan GC, et al. Electron injection into organic semiconductor devices from high work function cathodes. Proc Natl Acad Sci USA 2008;105:12730–5.
[52] Seo JH, Gutacker A, Walker B, Cho S, Garcia A, Yang R, et al. Improved injection in n-type organic transistors with conjugated polyelectrolytes. J Am Chem Soc 2009;131:18220–1.
[53] Li W, Hendriks KH, Wienk MM, Janssen RA. Diketopyrrolopyrrole polymers for organic solar cells. Acc Chem Res 2016;49:78–85.
[54] Kobaisi MA, Bhosale SV, Latham K, Raynor AM, Bhosale SV. Functional naphthalene diimides: synthesis, properties, and applications. Chem Rev 2016;116:11685–796.
[55] Wu Z, Sun C, Dong S, Jiang XF, Wu S, Wu H, et al. N-type water/alcohol-soluble naphthalene diimide-based conjugated polymers for high-performance polymer solar cells. J Am Chem Soc 2016;138:2004–13.
[56] Fang J, Wallikewitz BH, Gao F, Tu G, Muller C, Pace G, et al. Conjugated zwitterionic polyelectrolyte as the charge injection layer for high-performance polymer light-emitting diodes. J Am Chem Soc 2011;133:683–5.
[57] Duan C, Wang L, Zhang K, Guan X, Huang F. Conjugated zwitterionic polyelectrolytes and their neutral precursor as electron injection layer for high-performance polymer light-emitting diodes. Adv Mater 2011;23:1665–9.
[58] Duan CH, Zhang K, Guan X, Zhong CM, Xie HM, Huang F, et al. Conjugated zwitterionic polyelectrolyte-based interface modification materials for high performance polymer optoelectronic devices. Chem Sci 2013;4:1298–307.
[59] Page ZA, Duzhko VV, Emrick T. Conjugated thiophene-containing polymer zwitterions: direct synthesis and thin film electronic properties. Macromolecules 2013;46:344–51.
[60] Page ZA, Liu F, Russell TP, Emrick T. Tuning the energy gap of conjugated polymer zwitterions for efficient interlayers and solar cells. J Polym Sci: Polym Chem Ed 2015;53:327–36.
[61] Page ZA, Liu Y, Puodziukynaite E, Russell TP, Emrick T. Hydrophilic conjugated polymers prepared by aqueous horner–wadsworth–emmons coupling. Macromolecules 2016;49:2526–32.
[62] Zhou YH, Li FH, Barrau S, Tian WJ, Inganas O, Zhang FL. Inverted and transparent polymer solar cells prepared with vacuum-free processing. Sol Energy Mater Sol Cells 2009;93:497–500.
[63] Liu Y, Page ZA, Russell TP. Emrick T. Finely tuned polymer interlayers enhance solar cell efficiency. Angew Chem Int Ed 2015;54:11485–9.
[64] He Z, Zhong C, Huang X, Wong WY, Wu H, Chen L, et al. Simultaneous enhancement of open-circuit voltage, short-circuit current density, and fill factor in polymer solar cells. Adv Mater 2011;23:4636–43.
[65] He ZC, Zhong CM, Su SJ, Xu M, Wu HB, Cao Y. Enhanced power-conversion efficiency in polymer solar cells using an inverted device structure. Nat Photon 2012;6:591–5.
[66] He ZC, Xiao B, Liu F, Wu HB, Yang YL, Xiao S, et al. Single-junction polymer solar cells with high efficiency and photovoltage. Nat Photon 2015;9:174–9.
[67] Zhou G, Geng YH, Cheng YX, Xie ZY, Wang LX, Jing XB, et al. Efficient blue electroluminescence from neutral alcohol-soluble polyfluorenes with aluminum cathode. Appl Phys Lett 2006;89:233501, 1-4.
[68] Sun J, Zhu Y, Xu X, Lan L, Zhang L, Cai P, et al. High efficiency and high voc inverted polymer solar cells based on a low-lying HOMO polycarbazole donor and a hydrophilic polycarbazole interlayer on ITO cathode. J Phys Chem C 2012;116:14188–98.
[69] Liu S, Zhang K, Lu J, Zhang J, Yip HL, Huang F, et al. High-efficiency polymer solar cells via the incorporation of an amino-functionalized conjugated metallopolymer as a cathode interlayer. J Am Chem Soc 2013;135:15326–9.
[70] Wang J, Lin K, Zhang K, Jiang XF, Mahmood K, Ying L, et al. Crosslinkable amino-functionalized conjugated polymer as cathode interlayer for efficient inverted polymer solar cells. Adv Energy Mater 2016;6:1502563, 1-9.
[71] Park YJ, Cha MJ, Yoon YJ, Cho S, Kim JY, Seo JH, et al. Improved performance in n-type organic field-effect transistors via polyelectrolyte-mediated interfacial doping. Adv Electron Mater 2017;3:1700184, 1-7.
[72] Puodziukynaite E, Wang HW, Lawrence J, Wise AJ, Russell TP, Barnes MD, et al. Azulene methacrylate polymers: synthesis, electronic properties, and solar cell fabrication. J Am Chem Soc 2014;136:11043–9.
[73] Park JB, Isik M, Park HJ, Jung IH, Mecerreyes D, Hwang DH. Polystyrene-block-Poly(ionic liquid) copolymers as work function modifiers in inverted organic photovoltaic cells. ACS Appl Mater Interfaces 2018;10:4887–94.
[74] Liu Y, Cole MD, Jiang YF, Kim PY, Nordlund D, Emrick T, et al. Chemical and morphological control of interfacial self-doping for efficient organic electronics. Adv Mater 2018;30:1705976, 1-8.
[75] Cole MD, Sheri M, Bielicki C, Emrick T. Perylene diimide-based ionene and zwitterionic polymers: synthesis and solution photophysical properties. Macromolecules 2017;50:7535–42.
[76] Liu Y, Sheri M, Cole MD, Yu DM, Emrick T, Russell TP. Transforming ionene polymers into efficient cathode interlayers with pendent fullerenes. Angew Chem Int Ed 2019;58:5677–81.
[77] Liu Y, Sheri M, Cole MD, Emrick T, Russell TP. Combining fullerenes and zwitterions in non-conjugated polymer interlayers to raise solar cell efficiency. Angew Chem Int Ed 2018;57:9675–8.
[78] Xiong S, Hu L, Hu L, Sun L, Qin F, Liu X, et al. 12.5% flexible nonfullerene solar cells by passivating the chemical interaction between the active layer and polymer interfacial layer. Adv Mater 2019;31:1806616, 1-7.
[79] Cheng P, Zhan X. Stability of organic solar cells: challenges and strategies. Chem Soc Rev 2016;45:2544–82.